Brain & Development 41 (2019) 443–451

BRAIN & DEVELOPMENT
Official Journal of the Japanese Society of Child Neurology

www.elsevier.com/locate/braindev

Original article

Serial MRI findings of acute flaccid myelitis during an outbreak of enterovirus D68 infection in Japan

Akihisa Okumura [a,*,1], Harushi Mori [b,1], Pin Fee Chong [c], Ryutaro Kira [c], Hiroyuki Torisu [d], Sawa Yasumoto [e], Hiroyuki Shimizu [f], Tsuguto Fujimoto [g], Keiko Tanaka-Taya [g], the Acute Flaccid Myelitis Collaborative Study Investigators

[a] Department of Pediatrics, Aichi Medical University, Nagakute, Aichi, Japan
[b] Department of Radiology, Graduate School and Faculty of Medicine, The University of Tokyo, Tokyo, Japan
[c] Department of Pediatric Neurology, Fukuoka Children's Hospital, Fukuoka, Japan
[d] Department of Pediatrics, Fukuoka Dental College Medical and Dental Hospital, Fukuoka, Japan
[e] Medical Education Center, Fukuoka University School of Medicine, Fukuoka, Japan
[f] Department of Virology II, National Institute of Infectious Diseases, Tokyo, Japan
[g] Infectious Disease Surveillance Center, National Institute of Infectious Diseases, Tokyo, Japan

Received 5 October 2018; received in revised form 21 November 2018; accepted 6 December 2018

Abstract

Objecive: To clarify the neuroimaging findings of children with acute flaccid myelitis during an outbreak of EV-D68 infection.

Methods: We performed a detailed review of the spinal and cranial MRI results of 54 children with acute flaccid myelitis. We focused on the range of longitudinal lesions, the localization and appearance of lesions within a horizontal section, Gadolinium-enhancement, and changes over time.

Results: All children had longitudinal spinal lesions involving central gray matter. Twenty-six children had lesions spanning the entire spine. Six of them had weakness in all limbs, whereas seven had weakness of only one limb. Thirty-eight children had lesions in both gray and white matter and limb weakness tended to be more severe in these children. During the acute period, spinal lesions showed bilateral ill-defined widespread T2 hyperintensity. During the subacute period, lesions were well defined and confined to the anterior horn. The distribution of limb weakness was correlated with the appearance of lesions during the subacute period. Gadolinium enhancement was performed in 37 children, and enhancement was seen in the cauda equina in 29 children. Enhancement was infrequent within 2 days after onset but was seen in almost all children thereafter. Twenty-two children had brainstem lesions continuous with spinal lesions.

Conclusion: Extensive longitudinal spinal lesions were characteristic in children with acute flaccid myelitis. Lesions were usually bilateral and widespread during the acute period, whereas localization to the anterior horn could become obvious. Although enhancement of the cauda equina was often observed, its appearance was sometimes delayed.

Keywords: Longitudinal spinal lesions; Outcome; Serial changes; Brainstem; Gadolinium-enhancement

1. Introduction

Acute flaccid myelitis (AFM) is characterized by acute onset flaccid paralysis in association with spinal

* Corresponding author at: Department of Pediatrics, Aichi Medical University, 1-1 Yazako Karimata, Nagakute, Aichi 480-1195, Japan.
E-mail address: okumura.akihisa.479@mail.aichi-med-u.ac.jp (A. Okumura).
[1] Indicates equally contributing authors.

https://doi.org/10.1016/j.braindev.2018.12.001

motor neuron involvement. AFM was highlighted by the cluster coinciding with a nationwide outbreak of enterovirus D68 (EV-D68) in the USA in 2014 [1–5]. Several European authors have also reported patients with AFM associated with virologically confirmed EV-D68 infection [6–9], and an occurrence of AFM during an outbreak of EV-D68 infection was reported in Argentina [10]. Moreover, EV-D68 has been identified in patients with respiratory diseases throughout the world [6,8,9]. In Japan, a cluster of AFM, along with an outbreak of respiratory disease associated with EV-D68, was noted in autumn 2015 [11]. Event-based surveillance was initiated under special provision of the Infectious Diseases Prevention Law in September 2015. The AFM collaborative study investigators, supported by the Ministry of Health, Labor, and Welfare of Japan, analyzed the clinical characteristics and prognostic factors of AFM that were temporally correlated with an EV-D68 outbreak in Japan occurring in autumn 2015 [12].

During this national survey, neuroimaging data were obtained for central review. Reports of neuroimaging findings of AFM coinciding with EV-D68 outbreaks are limited, although a case series has been reported from the USA [13]. Here, we report the neuroimaging findings in children with AFM during an outbreak of EV-D68 infection occurring in autumn 2015 in Japan.

2. Methods

The study population was derived from a cohort of our previous nationwide survey of AFM patients in Japan admitted between August 1, 2015 and December 31, 2015 [12]. In this study, patients fulfilling all the following conditions were chosen from those recruited by the provisional acute flaccid paralysis surveillance commencing on October 21, 2015.

1) Patients with flaccid paralysis necessitating hospitalization $\geq$24 h.
2) Onset with acute focal limb weakness.
3) Evidence of spinal lesions.
4) Age $\leq$ 15 years.
5) Exclusion of other spinal disorders, including acute disseminated encephalomyelitis, neuromyelitis optica spectrum disorders, and Guillain–Barré syndrome.

The clinical manifestations of the patients have been reported elsewhere [12]. In our previous study, 59 of 115 patients identified by event-based surveillance were finally diagnosed with AFM. In the present study, we focused on the MRI findings of children (age $\leq$ 15 - years) with AFM, and excluded five patients from the previous cohort: one child with no obvious spinal lesions (Case 42) and four adults (Cases 54, 56, 59, and 77). Oral or written consent was obtained from all patients or their guardians, and ethical approval for this study was granted by the Ethics Committee of National Institute of Infectious Diseases of Japan (No. 655).

MRI using various sequences and parameters was performed at the hospital to which the patient was admitted. Spinal and cranial MRI data were obtained for central review. This study primarily evaluated MRI within 8 weeks after the onset of limb weakness. We focused on the following items: range of longitudinal lesions, localization and appearance of lesions within a horizontal section, gadolinium enhancement, and their changes over time. First, two reviewers (AO and HM) specializing in pediatric neuroimaging independently interpreted the MRI results. Then, a consensus on the interpretation was reached after discussion. The range of spinal longitudinal lesions was divided into four groups: entire, lesions from the cervical through the lumbar spine; cervical, lesions within the cervical spine; cervicothoracic or thoracic, lesions in the thoracic spine with or without lesions in the cervical spine; and thoracolumbar, lesions from the thoracic through the lumbar spine. Localization of lesions was divided into two groups; gray and white matter and gray matter alone. The appearance of lesions was divided into three groups; bilateral ill-defined widespread, bilateral well-defined anterior horn, and unilateral well-defined anterior horn. These items were sometimes difficult to determine due to lack of sufficient MRI acquisition and/or artifacts, such as body movement, and were classified as undetermined in such cases.

Motor function was assessed by a manual muscle strength test (MMT) and graded according to the Medical Research Council scale [14]. Overall MMT score was calculated from the sums of the average muscle strengths in each paralyzed extremity divided by the number of affected limbs. In our previous study, improvement of motor function was classified using a four-level system: complete, grade 5 on MMT score; good, two or more grades of MMT score recovery or grade 4 on MMT score; fair, slight improvement; and poor, no improvement. All patients with neurological sequelae were re-evaluated after $\geq$6 months.

We performed statistical analyses to compare the differences in several clinical variables according to MRI findings. We used the chi-square and Kruskal-Wallis tests to compare categorical and numerical variables, respectively. When the chi-square test revealed a significant difference, adjustment residual analysis was performed to identify the variables with a significant difference according to the groups. Statistical analyses were performed using EZR ver. 1.33 software (available at http://www.jichi.ac.jp/saitama-sct/SaitamaHP.files/statmed.html) [15]. In all analyses, $P < 0.05$ was taken to indicate statistical significance.

3. Results

3.1. Clinical features

The study population consisted of 54 children (32 males and 22 females). Their median age was 4 years (range, 0–12 years). EV-D68 infection was proven by reverse-transcription polymerase chain reaction in 7 children (Supplementary Table 1) [12]. Enteroviruses were detected in other two patients by pan-enterovirus real-time PCR. None of them could be typed because the amount of virus genomes was insufficient. The patterns of limb weakness were as follows: all extremities, $n = 9$; bilateral upper extremities (UEs) and one lower extremity (LE), $n = 1$; one UE and bilateral LEs, $n = 2$; bilateral UEs, $n = 1$; bilateral LEs, $n = 19$; ipsilateral UE and LE, $n = 1$; one UE, $n = 14$; and one LE, $n = 7$. Asymmetry of limb weakness was seen in 38 children. Seven children had cranial nerve dysfunction, 14 had neurogenic bladder/bowel, 10 had focal paresthesia, 6 had neck stiffness, and 5 had altered mental status.

3.2. Spinal MRI

By definition, spinal lesions were observed in all 54 children. In total, 115 spinal MRI studies were performed in 54 children within 8 weeks after the onset of limb weakness. The initial spinal MRI was performed 0–38 days (median, 5 days) after the onset. Two or more spinal MRI studies were performed in 43 children.

All children had longitudinal spinal lesions involving the central gray matter (Fig. 1). Longitudinal lesions were always observed in the initial spinal MRI regardless of the days after the onset of flaccid paralysis. The range of spinal lesions is shown in Table 1. In 8 children, the range of spinal lesions was difficult to determine due to insufficient MRI acquisition. Twenty-six children had lesions in the entire spine. The distribution of limb weakness was not always correlated with that of spinal lesions. Only six of 26 children with entire spinal lesions had weakness in all limbs, whereas seven had weakness in one limb. One of 8 children with lesions confined to the cervical spine had weakness in all limbs. Neurogenic bladder/bowel was observed in 14 children, and lesions in the lumbar spine were observed in 12 of these patients (entire spinal lesions, $n = 7$; thoracolumbar lesions, $n = 5$). No other clinical variables were correlated with the range of longitudinal spinal lesions.

The localizations of lesions on the initial spinal MRI are shown in Table 2. In 5 children, the localizations of spinal lesions were difficult to determine. Thirty-eight children had lesions in both the gray and white matter. Although there were no significant differences, 3- or 4-limb weakness was exclusively observed in children with lesions in both the gray and the white matter. There were no significant differences in other clinical variables according to the localization of spinal lesions.

Serial changes in spinal lesions are shown in Table 3. During the first week after onset, spinal cord lesions showed bilateral ill-defined widespread T2 hyperintensity without asymmetry (Fig. 1). During the second week, lesions tended to be confined to the anterior horn. After the third week (subacute period), lesions were well defined and confined to the anterior horn of one or both sides (Fig. 1). The side of the lesions coincided with that of limb weakness in children with unilateral well-defined anterior horn lesions. Supplementary Table 2 shows associations between the appearance of lesions during the subacute period and the range of longitudinal lesions and distribution of limb weakness. There was no relationship between the appearance of lesions during the subacute period and the range of longitudinal lesions. In contrast, the distribution of limb weakness was correlated with the appearance of lesions during the subacute period; bilateral lesions were significantly more frequent in children with weakness in all UEs and LEs, whereas unilateral lesions were more frequent in children with weakness in one UE or one LE. Unilateral lesions were invariably associated with asymmetry of limb weakness.

Gadolinium enhancement was performed in 37 children at least once, and enhancement was observed in 33 of them. Enhancement in the cauda equine, mostly predominant in ventral roots, was observed in 29 children (Fig. 2), whereas enhancement in nerve roots and spinal parenchyma were infrequent. Cauda equina enhancement was present even in three children with no longitudinal lesions in the lumbar spine. Table 3 shows the results of enhancement according to the days after the onset of limb weakness. Enhancement was observed in only 4 of 10 children within 2 days, whereas enhancement was seen in almost all children thereafter (Fig. 2). Among six children with no enhancement on the initial MRI within 2 days after onset, two underwent follow-up spinal MRI showing cauda equina enhancement.

3.3. Cranial MRI

Cranial MRI was performed on 50 children. Two children had abnormalities in the cerebrum. One child had punctate high intensities in the bilateral basal ganglia and thalami on T2-weighted images, and the other showed high intensities in the white matter of the right frontal lobe on T2-weighted images. These lesions were clinically silent. No children had abnormalities in the cerebellum. Twenty-two children had brainstem lesions invariably continuous with spinal lesions (Supplementary Table 3). Brainstem lesions were observed from the midbrain through the medulla oblongata in one child, from the pons to the medulla in 3, and within the medulla in 18. Four of 22 children with brainstem

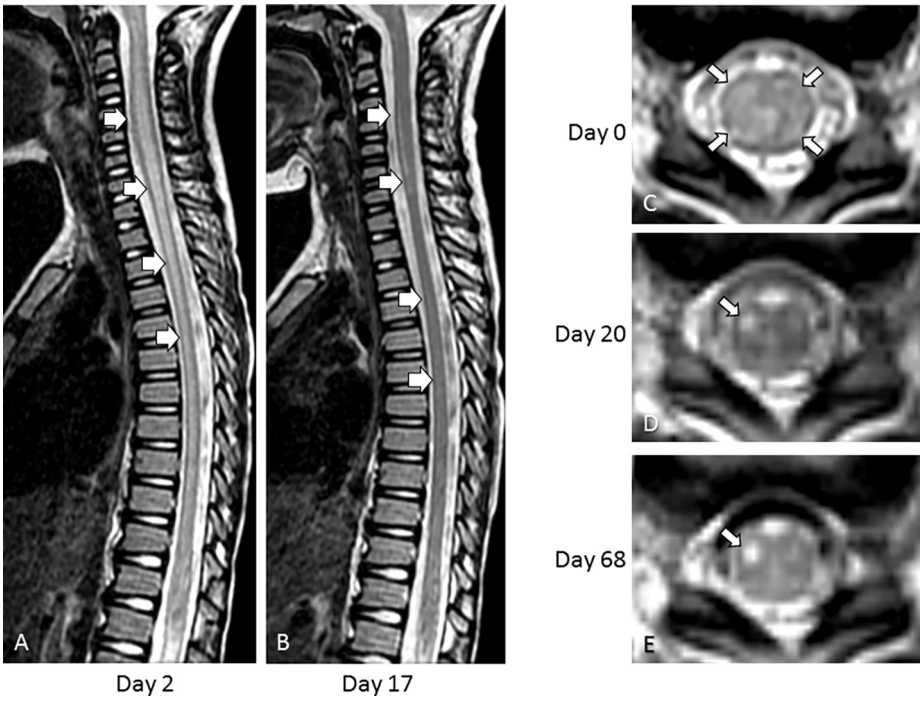

Fig. 1. Changes in spinal lesions over time. A and B. T2-weighted images of a 5-year-old child. The longitudinal lesion was ill defined and involved the entire central gray matter 2 days after the onset of limb weakness (A, arrows). The lesion became well defined and was confined to the anterior horn at 17 days after onset (B, arrows). The spinal cord was mildly atrophic. C–E. T2-weighted images of a 4-year-old child. An ill-defined lesion involving the entire gray matter and surrounding white matter on both sides was seen on the day of onset of limb weakness (C, arrows). A well-defined lesion was observed in the right anterior horn 20 days after onset (D, arrow). Slight high intensity was seen in the left anterior horn (D). The lesion in the right anterior horn became more clearly defined at 68 days after onset (E, arrow). Sample A was adopted from the reference #12. (For interpretation of the references to color in this figure legend, the reader is referred to the web version of this article.)

lesions had cranial nerve dysfunction involving VII, IX, X, XI, and XII nerves, and three had altered mental status. There were no significant differences in any of the clinical variables between children with and without brainstem lesions.

3.4. Outcomes and neuroimaging findings

Table 4 shows the relationships between the outcomes and the neuroimaging findings. The outcome was not correlated with the length of the spinal lesion, the localization of the lesion or the appearance of lesions during the subacute period.

4. Discussion

The present study revealed the neuroimaging features of children with AFM during the EV-D68 outbreak in 2015 in Japan. Extensive longitudinal spinal lesions were characteristic in children with AFM. Spinal lesions were predominantly located in the gray matter, whereas white matter involvement was frequent. Lesions were usually bilateral and widespread during the acute period, whereas localization to the anterior horn sometimes became obvious over time from onset. Enhancement of the cauda equina and/or nerve roots was often observed during the clinical course, whereas enhancement was infrequent during the first few days after onset. Brainstem lesions continuous to spinal lesions were common.

Extensive longitudinal spinal lesions were considered to be a characteristic feature of AFM in our cohort. About half the children with AFM had lesions spanning the entire spine, which was similar to previous reports regarding AFM [10,13,16]. Moreover, a majority of children with AFM had both gray and white matter lesions in our study, suggesting that the lesions in AFM may be very extensive. It is interesting that, unlike transverse myelitis, spasticity below the affected level and marked sensory level were not observed. Extensive longitudinal lesions can be observed in several spinal disorders, including neuromyelitis optica, longitudinally extensive transverse myelitis, and fibrocartilaginous embolism. Nichtweiß and Weidauer [17] proposed a scheme to categorize the imaging findings of acute myelopathy and stated that spinal MRI lesions in AFM are classified into the polio-like pattern characterized by the so-called "snake" or "owl's eye configuration." However, this configuration was uncommon in children with AFM.

Spinal MRI findings were altered over time from the onset. Within the first week after onset, all children had

Table 1
Range of longitudinal lesions.

	Range of longitudinal lesions					P value
	Entire (N = 26)	Cervical (N = 8)	Cervicothoracic or thoracic (N = 3)	Thoracolumber (N = 9)	Undetermined (N = 8)	
Age (years)*	4 (0–12)	3.5 (1–9)	2 (2–11)	4 (1–7)	3 (0–10)	0.91
Sex (male : female)	14:12	7:1	3:0	4:5	7:1	0.083
Proven EV-D68 infection	5	1	0	0	1	0.61
CSF pleocytosis	23	5	3	7	7	0.42
Increased CSF protein level	12	3	1	5	3	0.92
Time from onset of limb weakness to MRI acquisition (days)*	4.5 (0–26)	11 (1–16)	3 (2–5)	2 (1–38)	5 (0–7)	0.89
Limb weakness						Not assessed
All UEs and LEs	6	1	0	1	1	
Bilateral UEs and one LE	1	0	0	0	0	
One UE and bilateral LEs	1	0	1	0	0	
Bilateral UEs	1	0	0	0	0	
Bilateral LEs	10	0	2	6	1	
Ipsilateral UE and LE	0	0	0	0	1	
One UE	4	6	0	1	3	
One LE	3	1	0	1	2	
Asymmetry of limb weakness	15	8	2	6	7	0.16
Focal paresthesia	6	0	1	2	1	0.58
Neurogenic bladder/bowel	7	0	1	5	1	Not assessed

EVD68: enterovirus D68, CSF: cerebrospinal fluid, UE: upper extremity, LE: lower extremity.
* Data are show as median (range).

Table 2
Localization of parenchymal lesions.

	Localization of parenchymal lesions			P value
	Gray and white matter (N = 38)	Gray matter alone (N = 11)	Undetermined (N = 5)	
Age (years)*	4 (0–12)	4 (2–11)	6 (3–7)	0.12
Sex (male : female)	20:18	7:4	5:0	0.12
Proven EV-D68 infection	5	2	0	0.60
CSF pleocytosis	32	8	5	0.38
Increased CSF protein level	15	7	2	0.36
Time from onset of limb weakness to MRI acquisition (days)*	5 (0–38)	3 (1–23)	5 (2–9)	0.92
Limb weakness				0.055
All UEs and LEs	9	0	0	
Bilateral UEs and one LE	1	0	0	
One UE and bilateral LEs	2	0	0	
Bilateral UEs	1	0	0	
Bilateral LEs	13	3	3	
Ipsilateral UE and LE	1	0	0	
One UE	6	8	0	
One LE	5	0	2	
Asymmetry of limb weakness	26	8	4	0.85
Focal paresthesia	8	2	0	0.52
Neurogenic bladder/bowel	9	3	2	0.72

EVD68: enterovirus D68, CSF: cerebrospinal fluid, UE: upper extremity, LE: lower extremity.
* Data are show as median (range).

Table 3
Serial changes of appearance of spinal lesions and gadolinium-enhancement findings.

	Days after the onset of limb weakness					
	0–2 d	3–6 d	7–13 d	14–20 d	21–27 d	28–55 d
Appearance of spinal lesions	N = 19	N = 24	N = 21	N = 15	N = 20	N = 16
Bilateral ill-defined widespread	17	24	5	0	0	0
Bilateral well-defined anterior horn	0	0	11	6	11	9
Unilateral well-defined anterior horn	0	0	3	7	8	7
Disappearance	0	0	0	0	1	0
Undetermined	2	0	2	2	0	0
Gadolinium–Enhancement	N = 10	N = 11	N = 12	N = 5	N = 11	N = 8
Enhancement positive	4	10	12	5	10	8
Regions of enhancement						
Cauda equina	3	10	12	5	8	6
Ventral nerve roots	0	3	1	0	2	2
Dorsal nerve roots	0	3	1	0	2	0
Spinal parenchyma	1	0	0	0	0	1

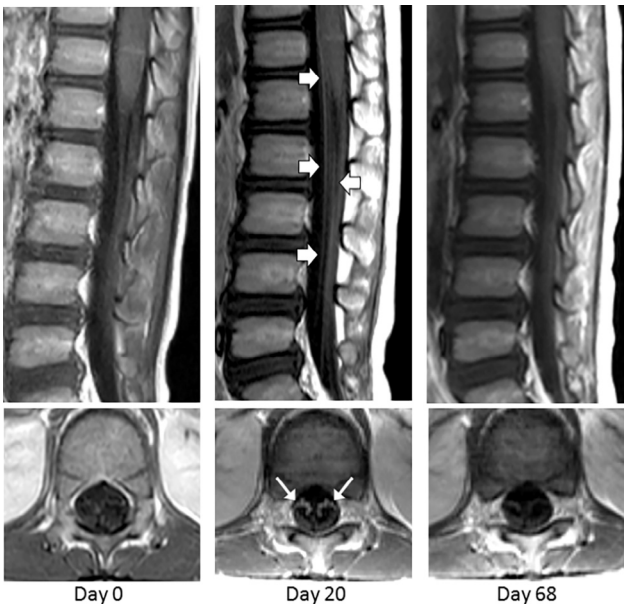

Fig. 2. Changes in gadolinium enhancement of the cauda equina over time. Gadolinium enhancement T1-weighted images of a 4-year-old child. No enhancement was observed on the day of onset of limb weakness (Left). Enhancement of the cauda equina predominantly in the ventral roots was seen at 20 days after onset (Middle, arrows). No enhancement was detected at 68 days after onset (Right). Lower middle sample was adopted from the reference #12.

widespread bilateral ill-defined lesions. Thereafter, the lesions gradually became confined to well-defined areas of the anterior horn on one or both sides during the subacute period. Serial changes in spinal MRI findings suggested that the lesions remaining during the subacute period may have indicated the most severely affected areas and that lesions during the acute period may include reversible components such as transient vasogenic edema. This hypothesis may be supported by the correlation of the distribution of limb weakness with the lesions during the subacute period. Bilateral lesions were more frequent in children with weakness in all four limbs, and unilateral lesions were more common in children with weakness in only one limb.

It is remarkable that the distribution of limb weakness was not always correlated with the extent of spinal lesions in our children with AFM, especially during the acute period. Some children with entire spinal lesions had weakness in only one limb. This also suggested that reversible components may be present in the T2-hyperitense spinal lesions in AFM. The core lesions were presumed to be located in the anterior horns, as indicated by the serial changes in spinal lesions. The discrepancy between the distribution of limb weakness and the range of spinal lesions may provide insight into the pathogenesis of AFM. AFM has been considered to be caused by direct viral pathogenic effects as shown by several experimental studies [18,19]. However, we presume that para infectious effects may also be related to the pathogenesis of AFM. Neuronal viral antigens and RNA detected in human autopsy cases were often more focal than expected from the extent and severity of inflammation [20]. Skeletal muscle infection has not been demonstrated in AFM in humans, indicating that virus entry via the peripheral motor nerves in skeletal muscle is unlikely. In our children with AFM, EV-D68 RNA was not detected in the cerebrospinal fluid. We postulate that the synergistic relationship between the direct viral pathogenic effects and some indirect effects may be involved in the pathogenesis of spinal lesions in children with AFM. The core lesions may be due to the direct viral pathogenic effects, and their indirect effects may contribute to the surrounding widespread lesions.

Cauda equina enhancement was frequent in our children with AFM. Enhancement was relatively infrequent during the first 2 days after the onset of limb weakness, and it was almost always observed thereafter. Delayed appearance of cauda equina was similar to that in the

Table 4
Outcome and spinal MRI findings.

	Outcome				P value
	Complete	Good	Fair	Poor	
Range of spinal lesions					
Entire (N = 26)	4	2	16	4	0.54
Cervical (N = 8)	1	2	4	1	
Cervicothoracic or thoracic (N = 3)	0	1	1	1	
Thoracolumber (N = 9)	0	3	4	2	
Localization of lesions					
Gray and white matter (N = 38)	6	6	23	3	0.15
Gray matter alone (N = 11)	0	3	5	3	
Lesions during the subacute period					
Bilateral (N = 26)	3	5	14	4	0.49
Unilateral (N = 18)	0	3	12	3	

report of Maloney et al. [13] and is likely a common feature of spinal lesions in children with AFM. It is remarkable that cauda equine enhancement was observed in some children even without apparent lumbar spine lesions. Nerve root enhancement has been suggested to be due to breakdown of the blood–nerve endothelial barrier after onset of anterior horn lesions [21]. The delayed appearance of enhancement suggests that nerve root enhancement may be better explained by parainfectious effects than by direct viral pathogenic effects.

Brainstem lesions were observed in about half the children in our study. Although the rate of brainstem lesions was smaller in our study than in the previous report [13], the radiological features of the brainstem lesions in our study were similar to those in the previous study; the lesions were located in the dorsal brainstem and were continuous to spinal lesions. Similar brainstem lesions were also observed in children with rhombencephalitis due to enterovirus 71 [22–24] and children with poliomyelitis [25]. A dissociation of the brainstem lesions and cranial nerve dysfunction was seen in our study. Only 4 of 22 children with brainstem lesions showed cranial nerve dysfunction, suggesting that transient vasogenic edema may be related to T2-hyperintensity of brainstem lesions.

Outcome was not correlated with the extent of the spinal lesions, the localization of the lesions, or the appearance of the lesions in the present study. Complete recovery occurred in 4 of 26 children with entire spinal lesions, whereas no children with cervicothoracic, thoracic, or thoracolumbar spinal lesions achieved complete recovery. Although 6 of 38 children with both gray and white matter lesions showed complete recovery, none of those with gray matter lesions alone recovered completely. The outcomes of children with bilateral lesions did not differ from those of children with unilateral lesions during the subacute period.

The main strength of our study was the number of children included in the analysis; this is the largest study of the neuroimaging findings of children with AFM reported to date. Nevertheless, this study had several limitations. First, the protocol and timing of MRI acquisition differed among the children due to the retrospective design of the study. Future studies should be performed in a prospective manner using an appropriate MRI acquisition protocol. Second, gadolinium enhancement was not performed in all children. Therefore, the evaluation of gadolinium enhancement was insufficient in our study. Third, the range of spinal lesions was not determined in some children because whole spinal MRI was not performed. This was because the entire spinal lesions were not expected in some children with weakness of one or two limbs. The necessity of whole spinal MRI was first indicated in the present study.

In summary, extensive longitudinal lesions were characteristic in children with AFM during the EV-D68 outbreak in Japan. The range of longitudinal lesions was more extensive than expected from the distribution of limb weakness. Spinal MRI including the whole spine is recommended in children with limb weakness suspected of having AFM. Gadolinium enhancement is also useful for diagnosis of AFM, although the possibility of delayed appearance of enhancement should be taken into consideration. An appropriate MRI acquisition protocol will be important for diagnosis and further studies of AFM. Neuroimaging findings of children with acute flaccid myelitis reported in this study would be useful for the expected protocol.

Acknowledgments

We thank the patients, their families, and members of the Japanese Society of Child Neurology for participation. We also thank epidemiologists and laboratory

experts at the prefectural and municipal health centers, local public health institutions, Japan association of prefectural and municipal public health institutes, and Ministry of Health, Labour and Welfare for providing information, laboratory data, and clinical samples under provisional AFP surveillance from August to December 2015.

Funding source

This work was supported by the Health and Labor Sciences Research Grant from the Ministry of Health, Labour and Welfare of Japan (grant number H25-Shinko-Shitei-006 to KT-T. and H28-Shinkogyosei-Ippan-007 to AO, HM, RK, HT, SY, HS, and KT-T), the Research Program on Emerging and Re-emerging Infectious Diseases from the Japan Agency for Medical Research and Development (AMED) (grant numbers 16fk0108205h0002 to AO, 40104400 to HS, and 40104402 to TF), and Fukuoka Children's Hospital Research Fund (to RK).

Potential conflicts of interest

The authors have no conflicts of interest relevant to this article to disclose.

Appendix A. Supplementary data

Supplementary data to this article can be found online at https://doi.org/10.1016/j.braindev.2018.12.001.

References

[1] Messacar K, Schreiner TL, Van Haren K, Yang M, Glaser CA, Tyler KL, et al. Acute flaccid myelitis: a clinical review of US cases 2012–2015. Ann Neurol 2016;80:326–8.
[2] Van Haren K, Ayscue P, Waubant E, Clayton A, Sheriff H, Yagi S, et al. Acute flaccid cyelitis of unknown etiology in California, 2012–2015. JAMA 2015;314:2663–71.
[3] Sejvar JJ, Lopez AS, Cortese MM, Leshem E, Pastula DM, Miller L, et al. Acute flaccid myelitis in the United States, August-December 2014: results of nationwide surveillance. Clin Infect Dis 2016;63:737–45.
[4] Messacar K, Schreiner TL, Maloney JA, Wallace A, Ludke J, Oberste MS, et al. A cluster of acute flaccid paralysis and cranial nerve dysfunction temporally associated with an outbreak of enterovirus D68 in children in Colorado. USA Lancet 2015;385:1662–71.
[5] Greninger AL, Naccache SN, Messacar K, Clayton A, Yu G, Somasekar S, et al. A novel outbreak enterovirus D68 strain associated with acute flaccid myelitis cases in the USA (2012–14): a retrospective cohort study. Lancet Infect Dis 2015;15:671–82.
[6] Dyrdak R, Grabbe M, Hammas B, Ekwall J, Hansson KE, Luthander J, et al. Outbreak of enterovirus D68 of the new B3 lineage in Stockholm, Sweden, August to September 2016. Euro Surveill 2016;21:30403.
[7] Pfeiffer HC, Bragstad K, Skram MK, Dahl H, Knudsen PK, Chawla MS, et al. Two cases of acute severe flaccid myelitis associated with enterovirus D68 infection in children, Norway, autumn 2014. Euro Surveill 2015;20:21062.
[8] Schuffenecker I, Mirand A, Josset L, Henquell C, Hecquet D, Pilorgé L, et al. Epidemiological and clinical characteristics of patients infected with enterovirus D68, France, July to December 2014. Euro Surveill 2016;21:30226.
[9] Holm-Hansen CC, Midgley SE, Fischer TK. Global emergence of enterovirus D68: a systematic review. Lancet Infect Dis 2016;16:e64–75.
[10] Ruggieri V, Paz MI, Peretti MG, Rugilo C, Bologna R, Freire C, et al. Enterovirus D68 infection in a cluster of children with acute flaccid myelitis, Buenos Aires, Argentina, 2016. Eur J Paediatr Neurol 2017;21:884–90.
[11] Korematsu S, Nagashima K, Sato Y, Nagao M, Hasegawa S, Nakamura H, et al. "Spike" in acute asthma exacerbations during enterovirus D68 epidemic in Japan: a nation-wide survey. Allergol Int 2018;67:55–60.
[12] Chong PF, Kira R, Mori H, Okumura A, Torisu H, Yasumoto S, et al. Clinical features of acute flaccid myelitis temporally associated with an enterovirus D68 outbreak: results of a nationwide survey of acute flaccid paralysis in Japan, August–December 2015. Clin Infect Dis 2018;66:653–64.
[13] Maloney JA, Mirsky DM, Messacar K, Dominguez SR, Schreiner T, Stence NV. MRI findings in children with acute flaccid paralysis and cranial nerve dysfunction occurring during the 2014 enterovirus D68 outbreak. Am J Neuroradiol 2015;36:245–50.
[14] Hislop HJ, Montgomery J. Daniels and Worthingham's muscle testing techniques of manual examination. Philadelphia: WB Saunders; 2002.
[15] Kanda R. Investigation of the freely available easy-to-use software 'EZR' for medical statistics. Bone Marrow Transplant 2013;48:452–8.
[16] Yoder JA, Lloyd M, Zabrocki L, Auten J. Pediatric acute flaccid paralysis: enterovirus D68-associated anterior myelitis. J Emerg Med 2017;53:e19–23.
[17] Nichtweiß M, Weidauer S. Differential diagnosis of acute myelopathies: an update. Clin Neuroradiol 2015;25(Suppl):183–7.
[18] Hixon AM, Yu G, Leser JS, Yagi S, Clarke P, Chiu CY, et al. A mouse model of paralytic myelitis caused by enterovirus D68. PLoS Pathog 2017;13 e1006199.
[19] Chan LG, Parashar UD, Lye MS, Ong FG, Zaki SR, Alexander JP, et al. Deaths of children during an outbreak of hand, foot, and mouth disease in Sarawak, Malaysia: clinical and pathological characteristic of the disease. Clin Infect Dis 2000;31:678–83.
[20] Wong KT, Badmanathan M, Ong KC, Kojima H, Noriyo N, Chua KB, et al. The distribution of inflammation and virus in human enterovirus 71 encephalomyelitis suggests possible viral spread by neural pathways. J Neuropathol Exp Neurol 2008;67:162–9.
[21] Nguyen C, Haughton V, Ho K, An HS, Myklebust JB, Hasegawa T, et al. Contrast enhancement in spinal nerve roots: an experimental study. Am J Neuroradiol 1995;16:265–8.
[22] Huang CC, Liu CC, Chang YC, Chen CY, Wang ST, Yeh TF. Neurologic complications in children with enterovirus 71 infection. N Engl J Med 1999;341:936–42.
[23] Chen CY, Chang YC, Huang CC, Lui CC, Lee KW, Huang SC. Acute flaccid paralysis in infants and young children with enterovirus 71 infection: MR imaging findings and clinical correlates. Am J Neuroradiol 2001;22:200–5.
[24] Jang S, Suh S, Ha SM, Byeon JH, Eun BL, Lee YH, et al. Enterovirus 71-related encephalomyelitis: usual and unusual magnetic resonance imaging findings. Neuroradiology 2012;54:239–45.
[25] Wasserstrom R, Mamourian A, McGary C, Miller G. Bulbar poliomyelitis: MR findings with pathologic correlation. Am J Neuroradiol 1992;13:371–3.